Structural and morphologic evolution of $Pt/Ba_{0.7}Sr_{0.3}TiO_3/Pt$ capacitors with annealing processes

Y. L. Qin,[a] C. L. Jia, and K. Urban
Institut für Festkörperforschung, Forschungszentrum Jülich GmbH D-52425 Jülich, Germany

R. Liedtke and R. Waser[b]
Institut für Werkstoffe der Elektrotechnik, Rheinisch-Westfälisch Technische Hochschule Aachen, D-52056 Aachen, Germany

(Received 19 November 2001; accepted for publication 13 February 2002)

The microstructure and chemistry of the as-grown, the postannealed and the forming-gas-atmosphere-treated $Pt/Ba_{0.7}Sr_{0.3}TiO_3/Pt$ capacitors are studied by means of high-resolution transmission electron microscopy and energy-disperse x-ray spectroscopy. It is found that the annealed $Ba_{0.7}Sr_{0.3}TiO_3$ films have larger grain size and more smooth top film-electrode interfaces. High-resolution images reveal the presence of disordered or amorphous regions at the interfaces in the $Ba_{0.7}Sr_{0.3}TiO_3$ film heated in the forming-gas atmosphere. These regions show a higher Ti/(Ba+Sr) ratio than the grain matrix. The effects of these amorphous regions on the electrical properties of $Ba_{0.7}Sr_{0.3}TiO_3$ films are discussed. © *2002 American Institute of Physics.* [DOI: 10.1063/1.1469683]

Thin films of $Ba_xSr_{1-x}TiO_3$ (BST) are promising candidates as high permittivity dielectrics for dynamic random access memories and other integrated capacitors.[1–3] However, in the technology of integration processes in traditional semiconductor circuits and devices, Pt/BST/Pt ferroelectric capacitors often suffer from, in particular, a large increase of the leakage current by more than four orders of magnitude after annealing in a strongly reducing atmosphere,[4,5] e.g., in a typical forming-gas anneal (N_2 95% and H_2 5%). In order to understand the underlying mechanism, we previously studied the electric properties of Pt/BST/Pt (metal-insulator-metal) (MIM) structures before and after annealing in atmospheres containing hydrogen or carbon monoxide by means of admittance spectroscopy.[6,7] The leakage current of the capacitors can be interpreted with respect to Schottky conduction. A decrease of Schottky barrier height by 0.4 eV after annealing in a reducing atmosphere was found. In this letter we report on a microstructural study of the Pt/BST/Pt ferroelectric capacitors by means of transmission electron microscopy (TEM). The emphasis is on the structure evolution of $Pt/Ba_{0.7}Sr_{0.3}TiO_3/Pt$ capacitors with annealing processes in order to understand the possible structure origin of the large increase of the leakage current.

The 130 nm $Ba_{0.7}Sr_{0.3}TiO_3$ films with a Ti/(Ba+Sr) ratio of 1.02 were deposited on $Pt/TiO_2/SiO_2/Si$ substrates by chemical solution deposition.[4,8] The 100 nm Pt top electrodes were deposited by rf magnetron sputtering.[7] Three samples were investigated: (A), the as-grown capacitor; (B), the postannealed capacitor under an oxygen atmosphere at $T=550-600\,^{\circ}C$ for 30 min; and (C), the capacitor after additional annealing at $T=450\,^{\circ}C$ under a forming-gas atmosphere (FGA). Cross-section TEM specimens were prepared by cutting the film-covered substrate wafers into slices. Two slices were glued together face to face. After conventional grinding and dimpling, these specimens were ion milled to perforation on a stage cooled by liquid nitrogen. Electron microscopy was performed with a Philips CM20 field-emission transmission electron microscope, operating at 200 kV. Chemical compositions of microregions were analyzed by energy dispersive x-ray spectroscopy (EDX) using a spot size of about 5 nm.

Electron diffraction and high-resolution electron microscopy (HREM) revealed that the bottom electrode Pt films are highly textured with the $\langle 111\rangle_{Pt}$ directions preferentially aligned parallel to the surface normal, whereas the BST films are not well oriented and the [100], [110], and [111] orientations in the growth direction of the films are all present in the three samples. Examination of the cross-sectional specimens of sample A [Fig.1(a)] shows that the BST film is composed of columnar grains with widths in the range of 30–50 nm, extending through the entire film thickness. The top Pt electrode layer has a similar columnar structure, but the sizes and orientations of grains have no relation to those of BST. The interface between the top Pt electrode and the BST film is quite rough, whereas the bottom interface is rather flat. The annealed BST films exhibit larger grains as shown in Fig. 1(b) (for sample B) and Fig. 1(c) (for sample C), compared with the as-grown one [Fig. 1(a)]. The top interfaces become smooth upon the annealing processes. No second phase or amorphous interlayer was observed at both interfaces in the first two samples. However, disordered or even amorphous-like regions were frequently found at both interfaces in sample C, which show a relatively bright contrast at both top and bottom BST-Pt interfaces in Fig. 1(c). The thickness of these amorphous regions varies from place to place along the interfaces and is in the order of several nanometers. The thicker amorphous region was usually found at the junctions of the grain boundaries and interface, and also in the areas of small grains. In the area shown in Fig. 1(c), the amorphous

[a]Author to whom correspondence should be addressed; electronic mail: y.qin@fz-juelich.de
[b]Also at: Institut für Festkörperforschung, Forschungszentrum Jülich GmbH D-52425 Jülich, Germany.

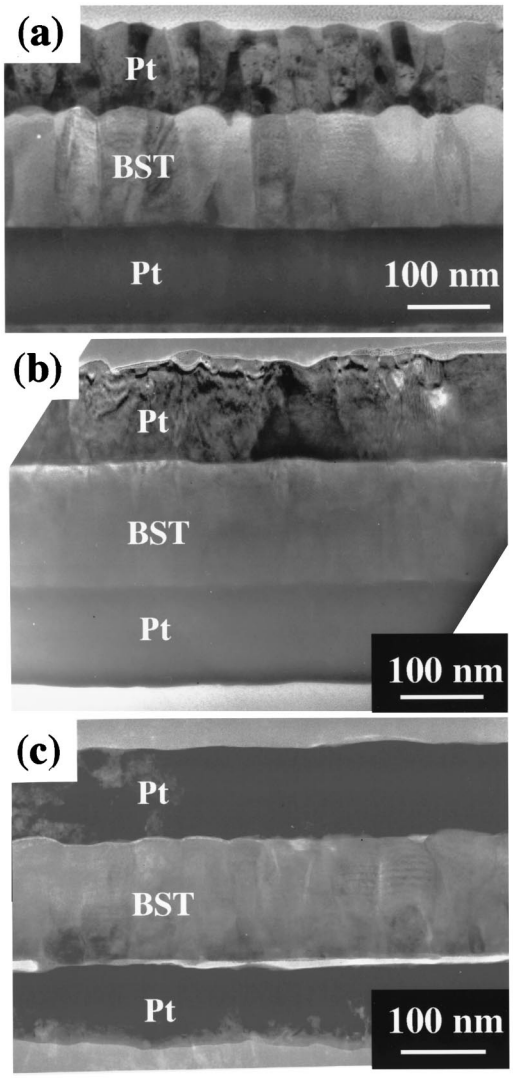

FIG. 1. Cross-section TEM bright-field images of Pt/BST/Pt capacitors: (a) as-deposited (sample A); (b) after optimized annealing at 600 °C (sample B); (c) additional annealing under the forming gas (sample C). Note that there are amorphous layers at the film-electrode interfaces of sample C, which show a relatively bright contrast.

region at the bottom interface is thicker than that at the top interface. We could also find the areas where the amorphous region at the top interface is thicker than that at the bottom interface. Figure 2 shows the images of the bottom interfaces (indicated by arrows) of the three samples at a higher magnification. The interfaces of samples A and B are flat and clean, whereas disordered area (marked by an arrow head) at the interface with amorphous contrast can be well recognized in sample C [Fig. 2(c)].

To identify this amorphous phase, EDX analysis was performed on sample C. Due to the difficulty in determining the absolute concentration of individual composition components, we investigated the changes in atomic ratio of Ti to (Ba+Sr) in the interface areas with respect to the crystalline film matrix. During the investigation, the EDX spectra from both BST film interior and the interface areas were acquired. Quantitative analysis averaging over several locations resulted in a Ti/(Ba+Sr) atomic ratio of 1.17. The same analysis was also carried out in the interface locations without the amorphous phase. No detectable difference was found in

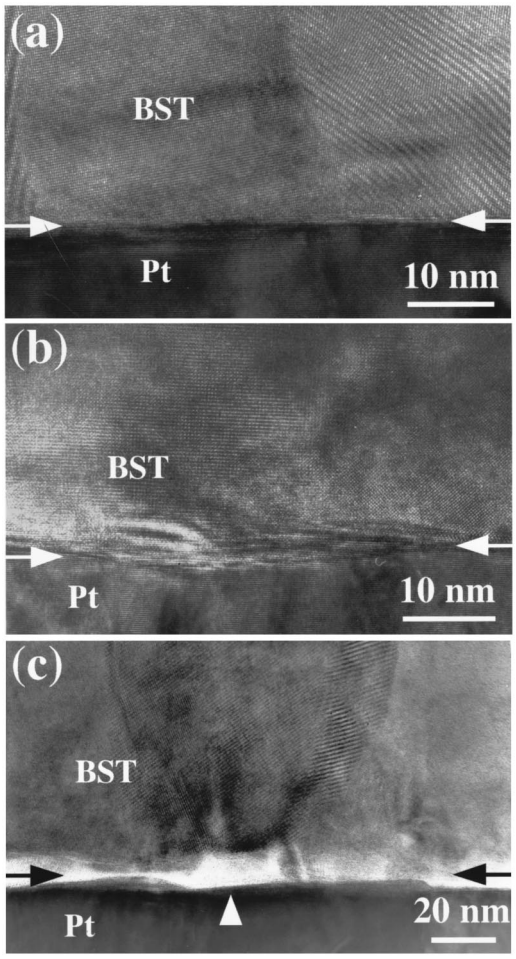

FIG. 2. Cross-sectional HREM images at low magnification of the BST/Pt bottom interfaces for (a) sample A; (b) sample B; and (c) sample C. Arrows denote the interfaces between the BST layer and the bottom electrode. An arrowhead marks an amorphous area at the interface in sample C.

comparison with the film interior. In Fig. 3, the ratio of Ti/(Ba+Sr) at the interface area and in the BST film interior is shown. It is evident that the interface areas with amorphous phase have a higher Ti content than the BST film matrix, whereas those without amorphous phase have nearly the same Ti content as the films. Therefore, the amorphous areas have a considerable amount of excess titanium.

It should be noted that the BST films studied are nons-

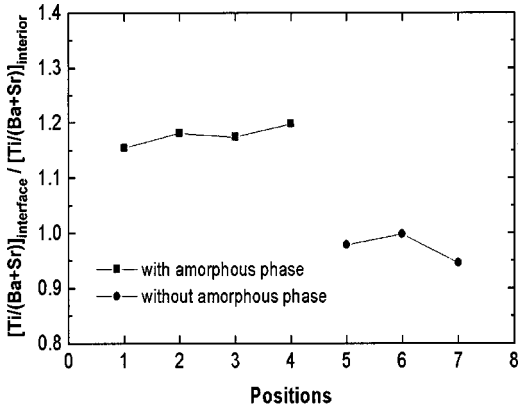

FIG. 3. The relative ratio of Ti/(Ba+Sr) between the interface and the film interior of sample C at different locations with (square) and without (circle) amorphous region.

toichiometric with a small titanium excess [Ti/(Ba+Sr) =1.02]. The mechanism for accommodation of excess Ti in the BST films with an average Ti/(Ba+Sr) ratio greater than unity has been studied recently by means of HREM and high-spatial resolution electron energy loss spectroscopy.[9–11] It has been reported that the excess Ti in BST films is accommodated through an increase in the concentration of Ba vacancies near and at the grain boundaries. As the Ti/(Ba +Sr) ratio increases, a Ti-rich amorphous phase evolves at some of the grain boundaries and multiple grain junctions. Analysis of structure images revealed that the volume fraction of the amorphous phase increases from about 1% to 5%–6% with an increase in Ti content from 52 to 53.4 at. %. The samples with less Ti (<52 at. %) contained no detectable amorphous phase. In addition, a systematic increase in the Ti/O ratio at the grain boundaries was found in a film containing 53.4 at. % Ti, while no such increase was detected for the specimen with 50.7 at. % Ti.[9] Our TEM observations of the as-grown and oxygen-postannealed BST film are consistent with the above results: no formation of Ti-rich amorphous regions at grain boundaries, triple junctions and the interfaces between BST and Pt electrodes, since the studied BST films only have 50.5 at. % Ti. However, amorphous regions were frequently observed at the interfaces in the FGA treated BST films. The mechanism of the formation of such amorphous phases can be explained as follows. During the annealing in a reducing atmosphere atomic oxygen diffuses easily out of the capacitor structure along the interfaces between BST film and Pt electrodes and the grain boundaries in the BST film. The oxygen vacancies concentrate at the interfaces and the grain boundaries leading to the formation of Ti-rich amorphous regions. It is known that hydrogen ions can also diffuse through the Pt layer and dissolve within the BST lattice forming an interface hydrogen layer during FGA.[12,13] However, the presence of the dissolved hydrogen cannot fully explain the increase in leakage current because of the comparable degradation of BST thin film capacitors in FGA and a CO-containing Ar atmosphere.[4]

The patchwork-like amorphous interface layer could have significant effects on the electrical properties of the Pt/BST/Pt MIM structure. It is known that the capacitance of a Pt/BST/Pt thin film capacitor can be modeled by an interface capacitance C_i and a bulk capacitance C_b in series, whereas the dielectric constant ϵ_i of the interface layer is assumed to be much lower than the bulk dielectric constant ϵ_b (samples A and B).[14] Then the total capacitance is given by $C_{\mathrm{ges}}{}^{-1}=2C_i{}^{-1}+C_b{}^{-1}$. Therefore it is comprehensible that the amorphous layer in sample C, which is assumed to have a low dielectric constant also, does not change the total capacitance C_{ges} dramatically.[7] Assuming an interface controlled Schottky conduction mechanism[15] it is obvious that a modification of the interface changes the Schottky barrier height. Two effects can be considered. First, the increase of the concentration of oxygen vacancies due to the annealing treatment in a reducing atmosphere, which are double charged donors, increases the internal electrical field at the Pt/BST interface. This will lower the Schottky barrier height due to the Schottky barrier lowering mechanism and the leakage current increases.[15] A strong accumulation of oxygen vacancies at the electrodes might result in the observed amorphization of the BST crystal lattice. Second, it is supposable that the electrical properties of the amorphous phase differ from the crystalline BST phase, and that further conduction mechanisms than the electron transport above a Schottky barrier-like tunneling or hopping in the amorphous phase might contribute to the total current flow.

In summary, the as-grown, the postannealed and the FGA treated Pt/BST/Pt capacitors are studied by means of HREM and energy dispersive x-ray spectroscopy. The postannealing treatment leads to an increased grain size of the $Ba_{0.7}Sr_{0.3}TiO_3$ films and a smoothness of the top film-electrode interfaces. The addition FGA treatment applied to the postannealing capacitors introduces the disordered or amorphous regions at the interfaces, which show a higher Ti/(Ba+Sr) ratio than the grain matrix. These amorphous regions are believed to be responsible for the increase of the leakage current.

[1] C. S. Hwang, S. O. Park, H.-J. Cho, C. S. Kang, S. I. Lee, and M. Y. Lee, Appl. Phys. Lett. **67**, 2819 (1995).
[2] J. S. Horwitz, W. Chang, A. C. Carter, J. M. Pond, S. W. Kirchoefer, D. B. Chrisey, J. Levy, and C. Hubert, Integr. Ferroelectr. **22**, 799 (1998).
[3] A. I. Kingon, S. K. Streiffer, C. Basceri, and S. R. Summerfelt, Mater. Res. Bull. **21**, 46 (1996).
[4] R. Liedtke, S. Hoffmann, M. Grossmann, and R. Waser, in *Proceedings of Semiconductor Advances for Future Electronics (SAFE99)* (Mierlo, The Netherlands, 1999), p. 281.
[5] D. Hadad, T.-S. Chen, V. Balu, B. Jiang, S. H. Kuah, P. McIntyre, S. Summerfelt, J. M. Anthony, and J. C. Lee, Integr. Ferroelectr. **17**, 461 (1997).
[6] G. W. Dietz, M. Schumacher, R. Waser, S. K. Streiffer, C. Basceri, and A. I. Kingon, J. Appl. Phys. **82**, 2359 (1997).
[7] R. Liedtke, M. Grossmann, and R. Waser, Appl. Phys. Lett. **77**, 2045 (2000).
[8] U. Hasenkox, S. Hoffmann, and R. Waser, J. Sol-Gel Sci. Technol. **12**, 67 (1998).
[9] S. Stemmer, S. K. Streiffer, N. D. Browning, and A. I. Kingon, Appl. Phys. Lett. **74**, 2432 (1999).
[10] I. Levin, R. D. Leapman, D. L. Kaiser, P. C. van Buskirk, S. Bilodeau, and R. Carl, Appl. Phys. Lett. **75**, 1299 (1999).
[11] I. Levin, R. D. Leapman, and D. L. Kaiser, J. Mater. Res. **15**, 1433 (2000).
[12] R. Waser, J. Am. Ceram. Soc. **71**, 58 (1988).
[13] W. Münch, J. Vac. Sci. Technol. B **14**, 2985 (1996).
[14] C. Basceri, S. K. Streiffer, A. I. Kingon, and R. Waser, J. Appl. Phys. **82**, 2497 (1997).
[15] C. S. Hwang, B. T. Lee, C. S. Kang, K. H. Lee, H.-J. Cho, H. Hideki, W. D. Kim, S. I. Lee, and M. Y. Lee, J. Appl. Phys. **85**, 287 (1999).